WHAT LIES BENEATH? COMPARING MODIS FRACTIONAL SNOW COVERED AREA AGAINST GROUND-BASED OBSERVATIONS UNDER FOREST CANOPIES AND IN MEADOWS OF THE SIERRA NEVADA

Mark S. Raleigh[1], Karl Rittger[2], and Jessica D. Lundquist[1]

ABSTRACT

Field observations are required to understand the potential errors in remotely sensed snow cover in forested areas. Here we compare fractional snow covered area (fSCA) from the Moderate Resolution Imaging Spectroradiometer (MODIS) snow covered area and grain size (MODSCAG) algorithm against ground-based observations during the 2010 water year. Three sites were selected with varying forest canopy density to quantify the impact of forest canopy on MODSCAG fSCA, which was corrected for vegetation using standard methods. The study was conducted at a 500m x 1000m plot in the forested Onion Creek Experimental Forest (1950m) of the North Fork American River basin (CA), and at 500m square plots in Tuolumne Meadows (2615m) and Dana Meadows (2985m) of Yosemite National Park in the Tuolumne River basin (CA). We used networks of ground temperature sensors in each study plot to monitor daily snow presence, and compared these to daily MODSCAG fSCA. A digital time-lapse camera at Tuolumne Meadows was used with a singular value decomposition to provide an independent check of fSCA. The results reveal the limitations of vegetation correction methods in forested areas, and the reasonable accuracy of MODSCAG under ideal conditions. (KEYWORDS: snow covered area, MODIS, forest canopy, ground observations)

INTRODUCTION

Remotely sensed observations of snow covered area (SCA) during the ablation season may be used to update streamflow forecast models (e.g., McGuire et al., 2006) or to allow seasonal reconstructions of past snow water equivalent (SWE) (e.g., Molotch, 2009). These advances are possible because the depletion of SCA contains information about maximum SWE and spring snowmelt rates (Liston, 1999). However, remote sensing of SCA is limited in forested regions, where the forest canopy obstructs the line-of-sight between the satellite and the area beneath the canopy, where snow may be present. In many mountainous basins around the world, the forested fraction may be extensive, thus limiting the potential value of remote sensing in understanding the snow hydrology of parts of these basins. For example, Klein et al. (1998) show that 40% of the snow zone in the mid-latitudes of the U.S. is covered by forests, presenting a significant and permanent challenge to remote sensing of snow. As an extreme example in the northern Sierra Nevada (i.e., Feather, Yuba, American basins), over 60% of the snow zone is covered by forests.

Ground-based validation of remotely sensed SCA from the Moderate Resolution Imaging Spectroradiometer (MODIS) is difficult because of the spatial resolution of the nadir (i.e., satellite directly overhead) footprint (500m) for land bands 1-7. Many studies have been conducted that compare MODIS SCA to SCA from remote sensing instruments with finer spatial resolution, such as 30m Landsat (e.g., Painter et al., 2009; Salomonson and Appel, 2004), but these are limited by the temporal resolution (16 days) of the Landsat sensor. Regardless of the instrument, satellite remote sensing has a suite of limitations, and these include cloud cover, off-nadir view angles, forest canopy obstruction, satellite noise, and issues related to temporal and spatial scaling of sampling. Additionally, many assumptions must be made about the physics of radiative transfer to convert observed radiance to reflectance across multiple wavelengths, as reflectance is ultimately required to map snow cover. Thus, ground-based validation is ideal to remove these challenges and to assess the accuracy of remotely sensed SCA. Additionally, ground-based observations may be the only way to assess fractional SCA (fSCA) errors under the forest canopy, where no satellite-based instrument can view the snow cover. Here we investigate the accuracy of fSCA retrievals from the MODIS snow covered area and grain size (MODSCAG) algorithm (Painter et al., 2009, Dozier et al., 2008, Dozier and Frew, 2009) in three areas with varying forest canopy density, and compare MODSCAG to ground-based observations.

Paper presented Western Snow Conference 2011
[1] Department of Civil and Environmental Engineering, Box 352700, University of Washington, Seattle, WA, 98195 mraleig1@uw.edu
[2] Bren School of Environmental Science and Management, University of California, Santa Barbara

SIERRA NEVADA STUDY AREAS

Sites were strategically selected in the California Sierra Nevada (Figure 1) to represent extremes in forest canopy density, in order to assess the impact of forest density on the accuracy of remotely sensed SCA. These study plots were sized to match MODIS grid cells (500m spatial resolution) at nadir view. Networks of ground temperature sensors were installed in these plots to produce ground-based observations of SCA (see **METHODS**). The study was conducted during water year 2010, beginning on 1 October 2009 and ending on 30 September 2010.

A 500m by 1000m study area (i.e., two neighboring MODIS cells) was established in the Onion Creek Experimental Forest in the headwaters of the North Fork American River basin (Figure 1a-b). The study area in Onion Creek has a mean forest canopy density of 65% (Table 1), based on 2001 National Land Cover Dataset canopy density maps (30m resolution). Onion Creek is covered by an old growth forest that includes red fir, white fir, sugar pine, Jeffrey pine, western white pine, lodgepole pine, incense-cedar, mountain hemlock, and western juniper (Tally, 1977). Immediately south of the Onion Creek study area, the forest opens up into a small (50,000 m^2) meadow. In this meadow, NOAA and Dessert Research Institute (DRI) weather stations monitor snow depth.

500m square study areas were also established in Dana Meadows and Tuolumne Meadows, which are subalpine meadows located at the headwaters of the Tuolumne River basin in Yosemite National Park. The Dana Meadows study area has a mean canopy density of 32%, while the Tuolumne Meadows study area has a mean canopy density of 23% (Table 1). The forested areas of these meadows are predominantly comprised of lodgepole pine. The California Department of Water Resources (CDWR) snow pillow and snow depth sensor at Dana Meadows are located in a clearing near the center of the 500m study domain. A CDWR snow pillow and snow depth sensor are located 1.4 km E/SE of the Tuolumne Meadows study area. At Tuolumne Meadows, a digital time lapse camera took 6 daily photographs of the meadow from Pothole Dome, located approximately 2.5km W/NW of the Tuolumne Meadows study area. These photographs provided an independent method of observing the depletion of SCA during May - June 2010. An algorithm (see **METHODS**) was developed to automatically detect snow presence in the sequence of images, and to estimate snow covered area from the sequence.

Table 1. Study areas in the Sierra Nevada, CA, with geophysical characteristics and available ground observations.

	Onion Creek	**Dana Meadows**	**Tuolumne Meadows**
River Basin	N.F. American	Tuolumne	Tuolumne
Latitude (N)	39° 16’	37° 54’	37° 52’
Longitude (W)	120° 21’	119° 15’	119° 22’
Elevation (m)	1950	2985	2615
Mean Forest Canopy Density, *F* (%)	65	32	23
Study area size	500m x 1000m	500m x 500m	500m x 500m
# of Ground Temperature Sensors	87 (UW)*	45 (UW)*	45 (UW)*
Snow Depth Sensors	2 (NOAA, DRI)*	1 (CDWR)*	1 (CDWR)*
Snow Pillows	None	1 (CDWR)*	1 (CDWR)*
Time Lapse Camera	None	None	1 (UW)*

**Acronyms of operators: UW = University of Washington, NOAA = National Oceanic and Atmospheric Administration, DRI = Desert Research Institute, CDWR = California Department of Water Resources.*

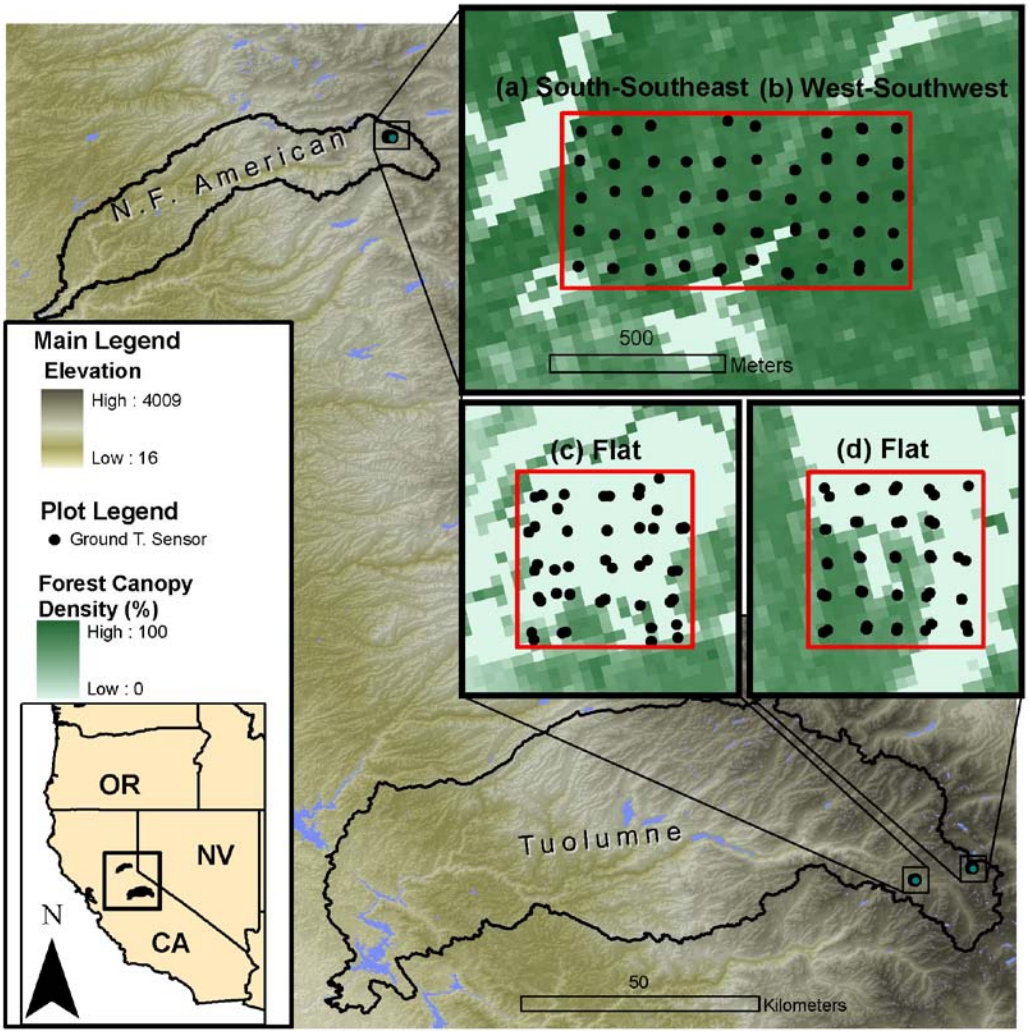

Figure 1. Study sites in the (a-b) Onion Creek Experimental Forest in the North Fork American River basin, and (c) Tuolumne Meadows and (d) Dana Meadows in Yosemite National Park, CA. The subplots (a-d) show the locations of buried temperature sensors in each study area, and the aspects of each plot are labeled: (a) south-southeast, (b) west-southwest, (c) flat, and (d) flat. Note that several sensor locations had two sensors installed in close proximity. The red box denotes the study size area, as listed in Table 1.

METHODS

MODIS Fractional Snow Covered Area: MODSCAG

Located on the Terra and Aqua satellites, the NASA MODIS instrument is an attractive remote sensing platform for hydrologists because each satellite provides nearly global coverage of the Earth every 1-2 days. Thus, with two satellites in orbit, daily or twice daily observations from the two MODIS instruments are commonly available, even at mid-latitude locations. MODIS is a scanning spectroradiometer that passive observes 36 spectral bands at 250m, 500m, and 1000m resolutions. Because the visible, near infrared, and shortwave infrared wavelengths, which are relevant to remote sensing of SCA, are observed at either 250m or 500m, gridded MODIS SCA products are created with 500m resolution (Table 2). However, it is important to note that the actual grid resolution is a function of satellite view angle, which fluctuates daily for each satellite. Dozier et al. (2008) comments that at a 55° view angle, a MODIS grid is 10 times larger than a MODIS grid cell at nadir view.

Among the available MODIS SCA retrieval algorithms (Table 2), the MODIS snow covered area and grain size (MODSCAG) algorithm was selected for this study because it is a “state of the art” retrieval algorithm and because ground-based observations are needed to quantify the errors of this relatively new algorithm. At each grid cell, MODSCAG solves for daily fractional SCA (fSCA) by using spectral mixture analysis to determine the best

combination of observed land surface "endmembers" (e.g., soil, rock, other, snow) that matches MODIS reflectance observations (Painter et al., 2009). Snow reflectance is estimated using a hemispherical directional reflectance factor and a discrete ordinates radiative transfer model. The MODSCAG algorithm is interpolated and smoothed in time at 500m on a pixel-by-pixel basis following Dozier et al. (2008) and Dozier and Frew (2009) to produce daily maps of fSCA across the Sierra Nevada. Interpolation and smoothing are used to account for data gaps and errors because of cloud cover and sensor viewing geometry. The stated lower limit of MODSCAG is 15% fSCA.

Table 2. Available MODIS snow covered area (SCA) retrieval algorithms and corresponding literature.

Algorithm	**Citations**
MOD10A1 Binary SCA	Hall et al. (2001)
MOD10A1 Fractional SCA	Salomonson and Appel (2004), Salomonson and Appel (2006)
MODSCAG Fractional SCA	Painter et al. (2009), Dozier et al. (2008), Dozier and Frew (2009)

Vegetation Corrections Applied to MODSCAG

Gridded products of remotely sensed fSCA are created based on the land surface that is viewable by the remote sensing instrument. In areas with forest canopy, the canopy may obstruct the land surface below the canopy, and the instrument may only "see" snowpack through canopy gaps and snowpack located in forest clearings. Other studies have applied corrections to fSCA products in forested grid cells by adjusting the fSCA time series by the viewable gap fraction of that grid cell (e.g., Liu et al., 2004; Durand et al., 2008; Molotch and Margulis, 2008). Here we use the same vegetation correction method for MODSCAG:

$$fSCA_{corrected} = \frac{fSCA_{MODSCAG}}{1-F} \qquad fSCA_{corrected} \leq 1.0, \quad F<1$$

where $fSCA_{corrected}$ is the fractional SCA corrected for vegetation, $fSCA_{MODSCAG}$ is the fractional SCA from the gridded daily 500m MODSCAG product, $1\text{-}F$ is the viewable gap fraction, and F is the fractional forest canopy density of the grid cell. This correction will uniformly increase the time series of fSCA as long as F>0. The value of F for each study area (Table 1) was held constant in time.

As identified by Durand et al. (2008), this vegetation correction assumes that the SCA under the forest canopy is proportional to the fSCA in the viewable areas (i.e., gaps, clearings, meadows). However, studies in both maritime and continental locations around the northern hemisphere show that snow accumulation and melt rates change based on the forest canopy density and type of tree (e.g., *Sierra Nevada*: Church, 1912; Kittredge, 1953; Anderson, 1963; *U.S. Pacific Northwest*: Storck et al., 2002; *Rocky Mountains*: Gary and Troendle, 1982, Troendle and Meiman, 1984; *Canadian Boreal forests*: Faria et al., 2000, Gelfan et al., 2004; *Russian forests*: Kuz'min, 1954, Kuz'min 1960; *Finnish forests*: Koivusalo and Kokkonen, 2002). Consequently, the assumption that fSCA under the forest canopy is equivalent to fSCA in meadows and clearings may not be robust. We employ this vegetation correction here to test whether fSCA under the canopy can be represented by fSCA in clearings.

Ground Temperature Observations

Under Sierra Nevada snowpack, near-surface ground temperature (T_g) is isothermal at 0°C because the low thermal conductivity of snow insulates the ground from cold fluctuations in air temperature, and because the temperature of snow cannot exceed the melting point. This feature presents an opportunity to observe snow presence by measuring T_g, as T_g observations will exhibit a "flat-line" at 0°C when snow is present (Tyler et al., 2008; Lundquist and Lott, 2008). The Maxim temperature data-logger iButton (model DS1922L) was used here to measure T_g every hour from August 2009 through July 2010. Networks of iButtons were deployed throughout each of the three study areas (Figure 1) and each iButton was installed at a depth of 2-5cm below the surface. 87 iButtons were successfully deployed and retrieved in Onion Creek, while 45 iButtons were deployed in each of the two Yosemite Meadows (Table 1). After retrieving the iButtons, all T_g time series were converted to time series of binary snow presence (0=snow-free, 1=snow). For each study plot, the number of iButtons reporting snow presence at each time step were summed and divided by the total number of iButtons in that study plot (Table 1) to produce a time series of fSCA.

A simple algorithm was developed to convert time series of T_g to snow presence at each measurement location. To automatically identify snow presence at a location in time, the algorithm required that two conditions

were met. First, T_g could not exceed a maximum value ($T_{g,max}$). Second, the algorithm either required that either T_g was constant over at least N time steps, or that the daily range in T_g did not exceed a threshold ($T_{range,max}$). Table 3 shows the threshold values used in this study. $T_{g,max}$ was set slightly higher than expected because some older iButtons were used, and these older sensors had some consistent bias in T_g observations but still exhibited the "flat line" in the presence of snow. The threshold values used in this automated algorithm appeared to reasonably translate snow presence from T_g.

Table 3. Threshold values used to convert hourly ground temperature to binary snow presence.

Maximum hourly ground temperature, $T_{g,max}$ (°C)	Number of hours with constant temperature, N (hrs)	Maximum diurnal fluctuation in ground temperature, $T_{range,max}$ (°C)
2.75	48	1.0

Time Lapse Imagery at Tuolumne Meadows

Previous studies have employed ground-based digital images to quantify SCA and to assess patterns of snow presence. Using digital camera images that were transformed into digital orthophotos, Hinkler et al. (2002) derived SCA depletion curves in Greenland. Through this approach, they found that the SCA depletion curves were controlled by initial snow amount and melt season air temperature. Floyd and Weiler (2008) used a time lapse camera to identify snow presence in tree canopies during rain-on-snow events in British Columbia. Schmidt et al. (2009) used two digital cameras to monitor SCA along different slopes in an alpine valley in Switzerland and found that topography could not explain all snow cover patterns. All of these previous approaches successfully implemented different algorithms to detect snow, but none utilized singular value decomposition (SVD) or Principal Components Analysis (PCA) to explain their systems in time and space (see Wall et al., 2003 for an introduction and overview of the SVD). For this study, we first created a threshold-based algorithm to automatically detect snow-covered pixels in each photo, and then used the SVD of this image sequence in order to derive an fSCA time series at Tuolumne Meadows.

Image Processing and Snow Detection Algorithm

The Tuolumne Meadows time lapse camera took photographs approximately every 4 hours every day during May and June 2010, but only photographs taken between 10AM and 2PM PST were used in this study for three reasons. (1) This time frame coincided with the overpass of the two MODIS satellites, as the Terra satellite typically passes over or near the Sierra Nevada at 11 AM PST while Aqua typically passes over at 1 PM PST. (2) This time frame coincides with the daily maximum height of the sun in the sky, and thus the period with minimal shadows and maximum brightness in the absence of clouds. (3) Restricting the photographic analysis to this time frame prevented noise from being introduced into the analysis due to lighting differences throughout the day. The camera was protected in casing, and secured to a wood board on the side of a tree, which held the camera still.

To make the analysis less data intensive, we reduced the data in each image with two steps. First, we reduced the resolution of each image by only keeping every third pixel in each row and column of every image. This pixel reduction did not visibly change the image to the human eye but allowed for faster processing with MATLAB. Second, we cropped each image to a narrow rectangular area that focused primarily on the western part of Tuolumne Meadows (Figure 2). For each photo, the red, green, and blue (RGB) matrices were added together to produce a "combined pixel matrix" (min: 0, max: 765). The combined pixel matrix was then normalized to the 0-255 range based on the minimum and maximum values in the combined pixel matrix; we call this the normalized combined pixel matrix (NCPM). The NCPM is essentially a gray-scale version of the original color image.

The algorithm was developed such that the histogram of the NCPM was used to identify snow-covered pixels in a scene and to identify cloudy scenes or scenes during active storms. Histograms of the color content in each NCPM were created. Histograms can be used to investigate the amount of similarly colored components in each image, therefore identifying the amount of snow and vegetation (Figure 2). Figure 2a shows the typical NCPM histogram for a clear sky day when the meadow was snow covered, which was distinctly different than the histogram for a stormy day with snow cover (Figure 2b) and a clear sky day with a snow-free meadow (Figure 2c). The histogram was bimodal during clear sky days with a snow covered meadow (Figure 2a). When there was a snowstorm (Figure 2b), the histogram values tended to migrate to the central values (in the 50-200 range). The darker, lower mode (i.e., forests) migrated to higher values because the presence of snowfall between the trees and the camera made the trees look whiter. Similarly, the whiter, upper mode (i.e., the snow cover on the meadow) migrated to lower values because the scene was less bright due to cloud cover. Stormy scenes (Figure 2b)

introduced noise into the algorithm, so these were automatically identified by the algorithm and removed. A scene was automatically classified as stormy if over 73% of the NCPM fell in the 50-200 range, and the mean pixel value of the NCPM exceeded 100 (Figure 2). Six scenes were removed from the analysis because of stormy conditions during the May-June period.

In development of the algorithm, a static RGB threshold for detecting snow cover (e.g., Floyd and Weiler, 2008) was deficient at detecting snow in scenes that were less bright. Bringing the threshold to a lower value caused reflective surface water to be incorrectly classified as snow. To overcome this challenge, a dynamic brightness threshold was incorporated into the algorithm. As a first step, the dynamic algorithm found only NCPM pixel values greater than 150, resulting in a distribution of pixels, D150. If the mean of D150 was greater than a whiteness threshold (185), then snow was detected for all pixels in the upper 99th percentile of D150. If the mean of D150 was less than or equal to the whiteness threshold, then only pixels that were 240 or greater were classified as snow. The snow detection algorithm translated each image into a binary snow matrix, where each pixel had a value of 1 (snow-covered) or 0 (snow-free). Visual comparison between each original image and the output binary snow matrix demonstrated that the algorithm reasonably detected snow presence in each image.

Singular Value Decomposition

The singular value decomposition (SVD) can be used to understand the underlying spatial and temporal structures within a data matrix. The SVD (e.g., Wall et al., 2003) is a powerful linear algebra tool used to investigate coefficients of the principal components of a possibly complex system. The SVD is equivalent to Principle Component Analysis (PCA) and Empirical Orthogonal Function (EOF) analysis. The SVD will produce three output matrices. Modes of energy contained in the system are identified and output into a singular value matrix [s], while matrices [u] and [v] explain the spatial (translational) and temporal (rotational) aspects of the system, respectively. The SVD orders these outputs such that the first mode of each matrix explains the most variance in the system, while subsequent modes explain less variance. By retaining these three matrices the dataset (or image) can be reproduced. Additionally, the SVD allows the dataset or image to be reconstructed with the primary modes, reducing the amount of information needed.

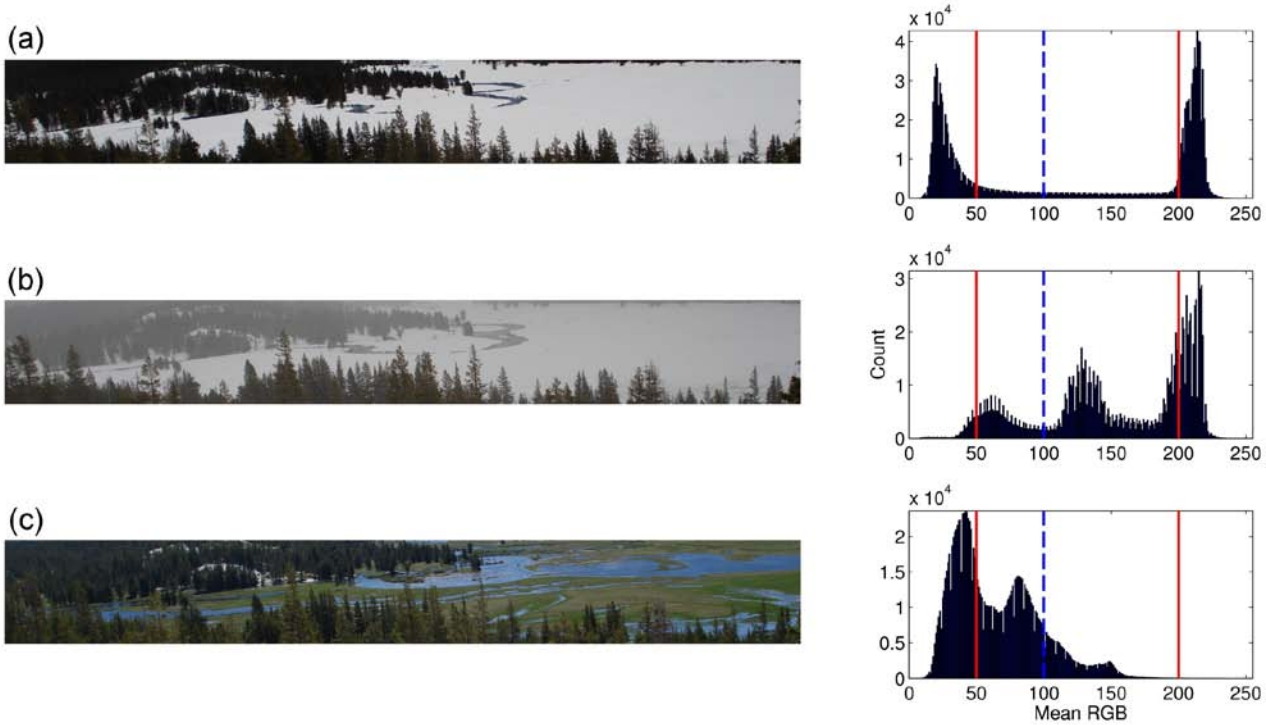

Figure 2. Three sample images from the time lapse camera at Tuolumne Meadows, with corresponding histograms of all pixels in each scene, averaged across red, green, and blue (RGB) values. Shown are (a) clear conditions with snow covered meadow, (b) stormy conditions with snow covered meadow, and (c) clear conditions with snow-free meadow. Solid and dashed lines in the histograms denote thresholds used to automatically map snow presence.

At each image (in time), the binary snow matrix was reshaped into a column vector and stored into a larger matrix (H). After this was conducted for all scenes, the SVD command was used with the H matrix as input. The rows of H corresponded to spatial location in the camera view, while the columns of H corresponded to time, as dictated by the day and time of each photo. Because the H matrix was established in this way, the resulting translational matrix (u) corresponded to spatial variations while the rotational matrix (v) corresponded to temporal variations. The first 5 modes of the SVD output of the Tuolumne Meadows camera explained 51% of the variance in the time-lapse sequence. The first spatial mode (Figure 3, top) clearly showed that the snow cover on the meadow explained the most variance in the sequence, while the subsequent four spatial moods reveal micro-scale patterns of snowmelt, movement of trees due to wind, and surface lighting patterns. The first temporal mode (Figure 4, top) characterizes how the snow cover depletes through time. To infer a time series of fSCA ("SVD-camera"), the absolute value of the first temporal mode was normalized to the 0-1 range producing an independent observation of fSCA depletion at Tuolumne Meadows.

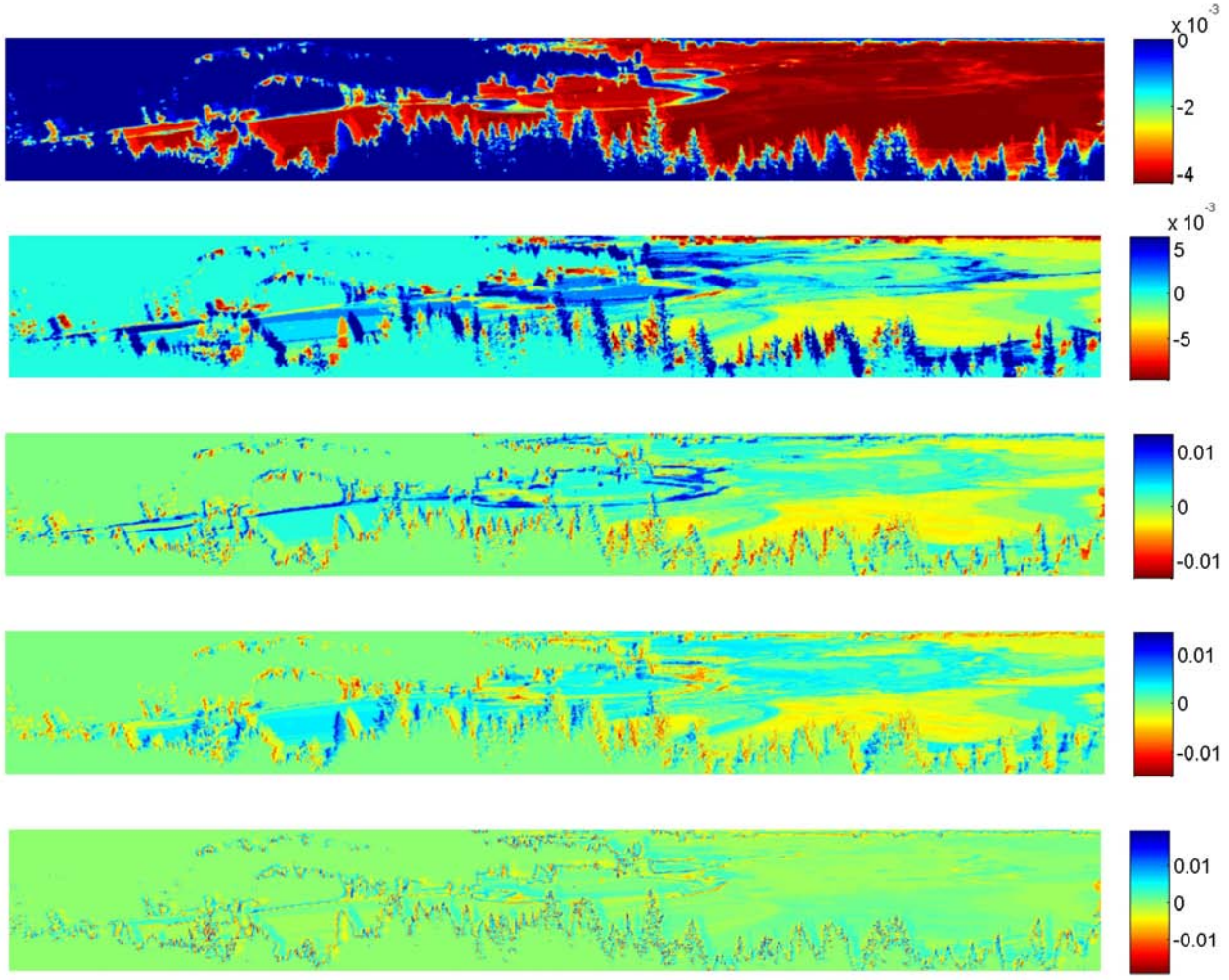

Figure 3. The first five spatial modes of variability from singular value decomposition of the time lapse image sequence at Tuolumne Meadows from 1-May to 30-June, 2010. The first mode was interpreted as snow presence, while subsequent modes reveal the strongest micro-scale patterns in the melting snow.

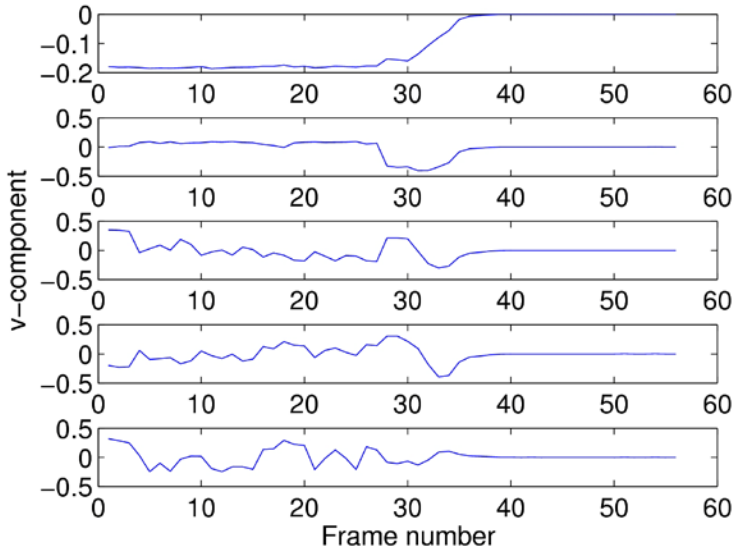

Figure 4. The first five temporal modes of variability from singular value decomposition of the time lapse image sequence at Tuolumne Meadows from 1-May to 30-June, 2010. The first mode (top) explains the evolution of snow presence in time, which was translated to a time series of fractional snow covered area.

FRACTIONAL SCA IN FORESTED ONION CREEK

In the Onion Creek study area, fSCA from the iButton network persisted longer than fSCA from MODSCAG (Figure 5). Although MODSCAG was increased by a factor of 3.33 with the vegetation correction (Equation 1), MODSCAG fSCA depleted completely in 1 day (31-May to 1-June), suggesting homogenous distributions of SWE. Ground observations from the iButton network did not indicate homogenous SWE, as the network reported 65% SCA on 1-June, 20% fSCA on 9-June, and 0% fSCA after 15-June. The timing of complete snow disappearance from MODSCAG agreed well with the point snow depth observations from NOAA and DRI. Because these snow depth sensors were located in an adjacent meadow, this agreement suggested that the signal was dominated by snow in clearings and gaps. The vegetation correction method (Equation 1) assumed that snow cover hidden under the forest canopy was equivalent to the viewable snow cover in the clearings and canopy gaps, but the ground-based results in Onion Creek do not support that assumption. The ground-based results indicate that snowpack persists longer under the forest canopy, and it is likely that lower melt rates allowed snow to persist longer in the forest.

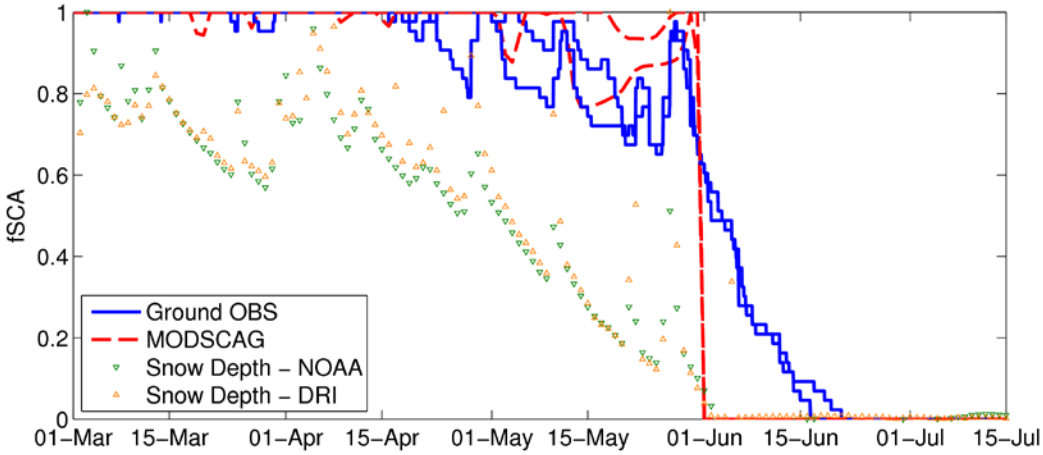

Figure 5. Snow presence at the Onion Creek study area (65% forest canopy density) during spring and summer 2010. Shown are fractional snow covered area (fSCA) time series as observed by distributed iButton ground temperature sensors and remotely sensed values from MODSCAG for 2 MODIS 500m pixels. Snow depth observations (scaled to the 0-1 range) in an adjacent meadow from the NOAA and DRI sensors are also shown.

FRACTIONAL SCA AT DANA MEADOWS

At the Dana Meadows study area, MODSCAG and the iButton network had reasonable agreement during the melt season, as was expected in a meadow (Figure 6). Root mean squared error in fSCA (iButtons vs. MODSCAG) during the second half of June was 0.15, and MODSCAG and the iButton network had a 2 day difference in observations of 20% fSCA. The two point observations of snow presence from the snow depth sensor and snow pillow showed snow disappearing completely when fSCA was near 20%. The detection limit of MODSCAG is 15% fSCA, which explains why the final ground observations of snow persist longer by a few days.

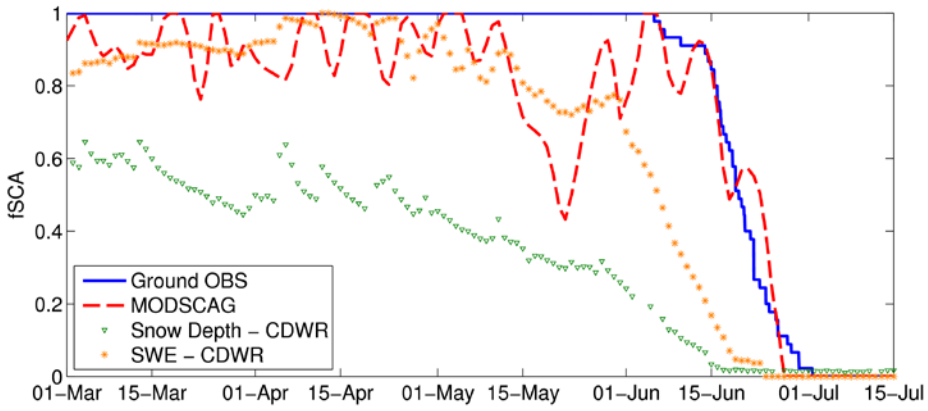

Figure 6. Snow presence at the Dana Meadows study area (32% forest canopy density) during spring and summer 2010. Shown are fractional snow covered area (fSCA) time series as observed by distributed iButton ground temperature sensors and remotely sensed values from MODSCAG. Snow depth observations and snow pillow SWE (both scaled to the 0-1 range) from the CDWR site in the middle of the study area are also shown.

FRACTIONAL SCA AT TUOLUMNE MEADOWS

We expected that MODSCAG would be most accurate at the Tuolumne Meadows study area, a flat meadow with light (23%) forest canopy density. However, MODSCAG fSCA depleted completely in 1 day (31-May to 1-June), which suggested homogenous SWE cover. The rapid disappearance of MODSCAG fSCA was 7 days earlier than ground observations from the iButton network and the SVD-camera (Figure 7). Observations of fSCA from the iButton network and the SVD-camera were in reasonable agreement and suggested patchy snow distributions (Figure 7). The timing of MODSCAG snow disappearance on 1-June compared well with point observations (snow pillow and snow depth sensor) at the Tuolumne Meadows CDWR site, located in a clearing.

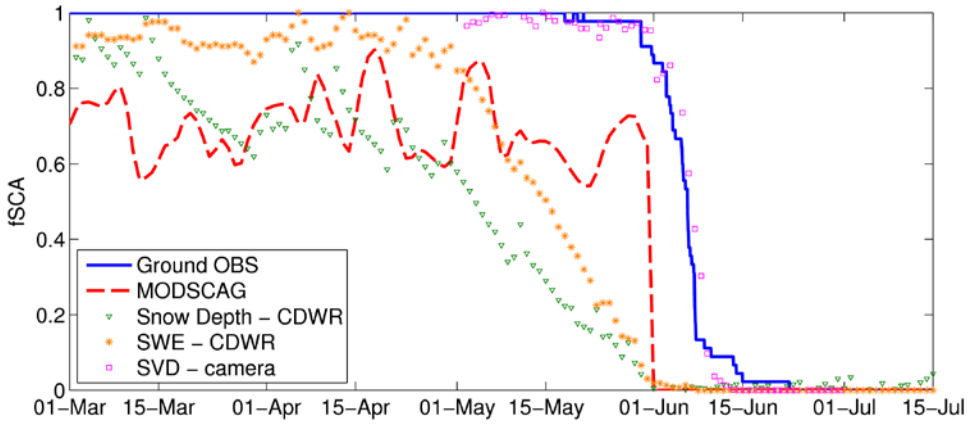

Figure 7. Snow presence at the Tuolumne Meadows study area (23% forest canopy density) during spring and summer 2010. Same as in Figure 6, but with the addition of fSCA from the first SVD mode of the time lapse images (SVD-camera). Snow depth observations and snow pillow SWE (both scaled to the 0-1 range) from the Tuolumne Meadows CDWR site (1.4km E/SE of the study area) are also shown.

Off-nadir satellite view angle and cloud presence during the first week of June appear to have caused the inaccuracy in MODSCAG fSCA at Tuolumne Meadows (Figure 8). The grid cell size was generally larger than 500m due to off-nadir view angles, and only 1 day in this period (5-June, Terra) had a nadir observation. Consequently, MODIS was generally observing an area larger than our study plot, and neighboring forested areas may have been observed in these shots. We also inspected the sky from the time-lapse imagery and looked for reduced incoming shortwave radiation (at Dana Meadows CDWR site) in order to assess which days had cloud cover. Clouds were present on 1-June, 3-June, and 4-June. The presence of clouds on these dates, combined with the off-nadir view angles of both satellites on 2-June resulted in 4 consecutive days with non-ideal conditions for MODIS (Figure 8). These results demonstrate that even in the absence of forest canopy, remotely sensed SCA can have inaccuracies due to view angle and cloud cover.

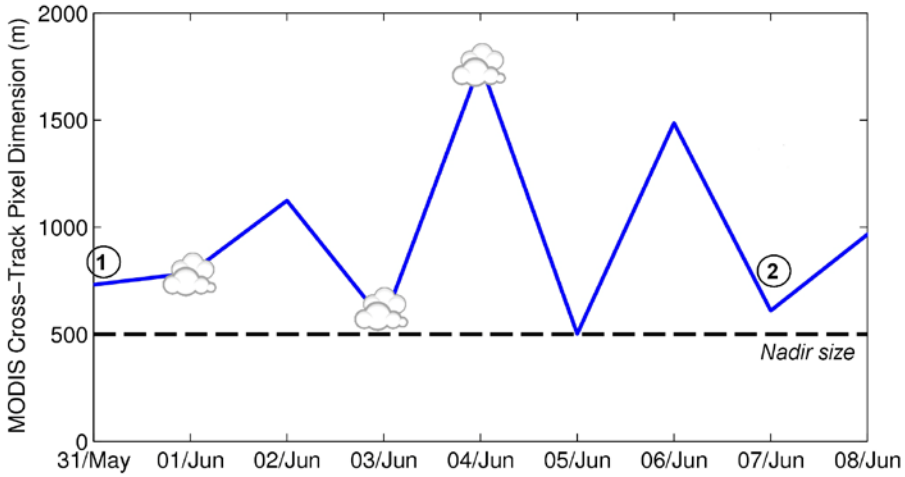

Figure 8. MODIS Terra cross track pixel size at Tuolumne Meadows from 31/May to 08/Jun 2010, relative to the nadir (500m) size. Shown are days with likely cloud presence (e.g., 01/Jun, 03/Jun, 04/Jun), which were inferred from radiation observations and time-lapse photos. From 31/May to 01/Jun (1) MODSCAG fSCA drops from 65% to 0% in one day and iButton fSCA = 87%. On 07/Jun (2) the iButton fSCA = 33%.

PRELIMINARY CONCLUSIONS

This study compared fSCA from MODSCAG against ground observations in three study areas with varying forest densities. The results at the forested Onion Creek suggest that methods of correcting remotely sensed SCA for vegetation cover should not assume that SCA under the canopy is equivalent to SCA in clearings. Results at Dana Meadows demonstrate the accuracy of the MODSCAG algorithm under more ideal conditions, while results at Tuolumne Meadows demonstrate that the accuracy of remotely sensed SCA in meadows can still be limited by off-nadir view angles and cloud cover.

ACKNOWLEDGMENTS

This work was supported by NASA Headquarters under the NASA Earth and Space Science Fellowship Program – Grant NNX09AO22H. Additional support was provided by the National Oceanic and Atmospheric Administration (NOAA) Hydrometeorological Testbed Project, under award NA17RJ1232. Special thanks to Courtney Moore for field work and collaboration with the time lapse photo analysis. Additional thanks to Brian Henn, and Nic Wayand for field work assistance. We would like to acknowledge and thank Randall Osterhuber and the Central Sierra Snow Lab for field support in the American River basin, and Jim Roche, Peggy Moore and the USGS for field support in Yosemite National Park. Special thanks to Steve for help with image optimization.

REFERENCES

Anderson, H.W. 1963. Managing California's snow zone lands for water. U.S.D.A. Forest Service Research Paper PSW-6. Pacific Southwest Forest and Range Experiment Station, Berkely, California.

Church, J.E. 1912. The conservation of snow: its dependence on forest and mountains. Scientific American Supplement 74, 152-155.

Dozier, J., T.H. Painter, K. Rittger, and J.E. Frew. 2008. Time-space continuity of daily maps of fractional snow cover and albedo from MODIS. *Adv. in Water Resour.* **31,** 1515-1526.

Dozier, J. and J. Frew. 2009. Computational provenance in hydrologic science: a snow mapping example. *Phil. Trans. R. Soc. A.* **367**, 1021-1033.

Durand, M., N.P. Molotch, and S.A. Margulis. 2008. Merging complementary remote sensing datasets in the context of snow water equivalent reconstruction. *Remote Sens. Environ.* **112**(3), 1212-1225.

Faria, D.A., J.W. Pomeroy, and R.L.H. Essery. 2000. Effect of covariance between ablation and snow water equivalent on depletion of snow-covered area in a forest. *Hydrol. Process.* **14**, 2683-2695.

Floyd, W. and M. Weiler. 2008. Measuring snow accumulation and ablation dynamics during rain-on-snow events: innovative measurement techniques. *Hydrol. Process.* **22,** 4805-4812.

Gary, H.L., and C.A. Troendle. 1982. Snow accumulation and melt under various stand densities in lodgepole pine in Wyoming and Colorado. U.S.D.A. Forest Service Research Note RM-417. Rocky Mountain Forest and Range Experiment Station, Fort Collins, Colorado.

Gelfan, A.N., J.W. Pomeroy, and L.S. Kuchment. 2004. Modeling forest cover influences on snow accumulation, sublimation, and melt. *J. of Hydromet.-Special Section*, **5**, 785-803.

Hall, D.K, J.L. Foster, V.V. Salomonson, A.G. Klein, and J.Y.L. Chien. 2001. Development of a technique to assess snow-cover mapping errors from space, *IEEE Trans. on Geoscience and Remote Sensing*. **39**(2), 432-438.

Hinkler, J., S.B. Pedersen, M. Rasch, and B.U. Hansen. 2002. Automatic snow cover monitoring at high temporal and spatial resolution, using images taken by a standard digital camera. *Int. J. of Remote Sensing*. **23**(21), 4669 – 4682.

Kittredge, J. 1953. Influence of forests on snow in the ponderosa-sugar pine-fir zone of the central Sierra Nevada. *Hilgardia* **22**, 1-96.

Klein, A.G., D.K. Hall, and G.A. Riggs. 1998. Improving snow cover mapping in forests through the use of a canopy reflectance model. *Hydrol. Process*. **12**. 1723-1744.

Koivusalo, H., and T. Kokkonen. 2002. Snow processes in a forest clearing and in a coniferous forest. *J. Hydrol*. **262**, 145-164.

Kuz'min, P.P. 1954. Influence of the forest on snow melt (in Russian). *Trans. State Hydrol. Inst.*, **42**(96), 3-68.

Kuz'min, P.P. 1960. Snow accumulation and methods of estimating snow water equivalent (in Russian). *Hydrometeoizdat*, 171 pp.

Liston, G.E. 1999. Interrelationships among snow distribution, snowmelt, and snow cover depletion: Implications for atmospheric, hydrologic, and ecologic modeling. *J. Appl. Meteorol*. **38**(10), 1474-1487.

Liu, J., R.A. Melloh, C.E. Woodcock, R.E. Davis, and E.S. Ochs. 2004. The effect of viewing geometry and topography on viewable gap fractions through forest canopies. *Hydrol. Process.* **18**, 3595-3607.

Lundquist, J.D., and F. Lott. 2008. Using inexpensive temperature sensors to monitor the duration and heterogeneity of snow-covered areas. *Water Resour. Res., Measurement Methods issue*. **44**, W00D16, doi:10.1029/2008WR007035.

McGuire, M., A.W. Wood, A.F. Hamlet, and D.P. Lettenmaier. 2006. Use of satellite data for streamflow and reservoir storage forecasts in the Snake River Basin. *ASCE J. of Water Res. Planning and Mgmt.*, **132**, 97-109.

Molotch, N.P. 2009. Reconstructing snow water equivalent in the Rio Grande headwaters using remotely sensed snow cover data and a spatially distributed snowmelt model. *Hydrol. Processes.* **23**(7), 1076-1089.

Molotch, N.P., and S.A. Margulis. 2008. Estimating the distribution of snow water equivalent using remotely sensed snow cover data and a spatially distributed snowmelt model: a multi-resolution, multi-sensor comparison. Adv. Water Resour. 31(11), 1503-1514.

Painter, T. H., K. Rittger, C. McKenzie, R. E. Davis, and J. Dozier. 2009. Retrieval of subpixel snow-covered area, grain size, and albedo from MODIS. *Remote Sens. Environ.* **113**, 868–879.

Salomonson, V.V. and I. Appel. 2004. Estimating fractional snow cover from MODIS using normalized difference snow index. *Remote Sens. Environ.* **89**(3), 351-360.

Salomonson, V.V. and I. Appel. 2006. Development of the Aqua MODIS NDSI fractional snow covered area algorithm and validation results. *IEEE Trans. on Geoscience and Remote Sensing*, **44**(7), 1747-1756.

Schmidt, S., B. Weber, and M. Winiger. 2009. Analyses of seasonal snow disappearance in an alpine valley from micro- to meso-scale (Loetschental, Switzerland). *Hydrol. Process.* **23.** 1041-1051.

Storck, P., D.P. Lettenmaier, and S.M Bolton. 2002. Measurement of snow interception and canopy effects on snow accumulation and melt in a mountainous maritime climate, Oregon, United States. *Water Resour. Res.* **38**(11), doi:10.1029/2002WR001281.

Tally, S.N. 1977. An ecological survey of the Onion Creek candidate Research Natural Area on the Tahoe National Forest, California. Unpublished manuscript on file, Pacific Southwest Forest and Range Experiment Station. Berkeley, CA. 65 p.

Troendle, C.A., and J.R. Meiman. 1984. Options for harvesting timber to control snowpack accumulation. Proceedings of the 52nd Western Snow Conference. Sun Valley, Idaho. pp. 86-97.

Tyler, S.W., S.A. Burak, J.P. McNamara, A. Lamontagne, J.S. Selker, and J. Dozier. 2008. Spatially distributed temperatures at the base of two mountain snowpacks measured with fiber-optic sensors. J. of Glaciology, 54(187), 673-679.

Wall, M.E., A. Rechtsteiner, and L.M. Rocha. 2003. Singular value decomposition and principal component analysis. Found in *A Practical Approach to Microarray Data Analysis*. D.P. Berrar, W. Dubitzky, and M. Granzow, eds. Kluwer: Norwell, MA, pp. 91-109.